Predicting tropical cyclone rapid intensification using the 37 GHz ring pattern identified from passive microwave measurements

Margaret E. Kieper[1] and Haiyan Jiang[1]

Received 26 April 2012; revised 28 May 2012; accepted 29 May 2012; published 6 July 2012.

[1] A distinctive satellite-derived precipitative ring pattern around the tropical cyclone (TC) center is found to be related to rapid intensification (RI). The ring pattern appears on the Naval Research Laboratory (NRL) 37 GHz passive microwave composite color product as a cyan color ring. The probability of RI is evaluated for cases with this ring pattern by reviewing images of the NRL product for 84 TCs during 2003–2007 in the Atlantic basin using 6-hourly National Hurricane Center (NHC) best track data. It is found that when combining the ring criterion with the Statistical Hurricane Prediction Scheme (SHIPS) RI Index (RII), the probability of RI almost doubled, indicating that both the ring and SHIPS RII contain independent information for RI prediction. A subjective technique for predicting RI is proposed using both the 37 GHz ring and the SHIPS RII. Both the probability of detection (POD) and the false alarm ratio (FAR) for the combined ring+SHIPS RII are lower than those for SHIPS RII alone (POD, 24% versus 77%, and FAR, 26% versus 66%) when treating every 6-hr synoptic time as a separate case. Since the method was initially developed for RI event-based forecasts, statistics based on 2003–2007 Atlantic RI events, which consist of a contiguous period where any 24-hour subset shows at least a 30 kt intensity increase, are also generated. The method captures 21 out of these 28 events and produces 2 false alarms, producing a POD of 75% and a FAR of 9%. **Citation:** Kieper, M. E., and H. Jiang (2012), Predicting tropical cyclone rapid intensification using the 37 GHz ring pattern identified from passive microwave measurements, *Geophys. Res. Lett.*, *39*, L13804, doi:10.1029/2012GL052115.

1. Introduction

[2] Although tropical cyclone (TC) track forecasts have been improved substantially during the past 20 years, little gain in accuracy of forecasting TC intensity, especially rapid intensification (RI), over the same period has been achieved [*Rappaport et al.*, 2009]. The physical processes associated with RI, which is usually defined as 24-h intensity increase ≥30 kt [*Kaplan and DeMaria*, 2003], remain unsolved. Favorable large-scale environmental conditions that are near-universally agreed to be necessary for TC intensification include: warm sea surface temperature (SST), high low- to mid-level moisture, and low vertical wind shear [*Merrill*, 1988]. *Kaplan et al.* [2010] showed that a RI prediction index based on only environmental parameters is skillful in the Atlantic and Northern East Pacific basins, while *Hendricks et al.* [2010] indicated that RI might be controlled by storm internal dynamics providing a favorable pre-existing environmental condition.

[3] The hot tower hypothesis [*Malkus et al.*, 1961; *Simpson et al.*, 1998] assumes that the latent heating release by those intense convective overshooting towers is crucial to TC intensification. Convective asymmetries [*Braun et al.*, 2006] and vortical hot towers [*Montgomery et al.*, 2006; *Molinari and Vollaro*, 2010] have also been indicated to be related to TC RIs. However, it has been indicated that the increase of the probability of RI for TCs with hot towers in the inner core is not substantial relative to the climatological mean [*Jiang*, 2012]. On the other hand, an alternative hypothesis to the hot tower hypothesis was developed in the early 1980s. It has been shown that symmetric heating was a major factor in most TC intensification through both theoretical [*Shapiro and Willoughby*, 1982; *Nolan and Grasso*, 2003] and observational studies [*Willoughby et al.*, 1982; *Willoughby*, 1990]. Recently, *Nguyen et al.* [2011] advance the idea that TC may vacillate between symmetric and asymmetric intensification through a modeling case study of Hurricane Katrina (2005). However, it is not clear whether the symmetric or asymmetric process leads the intensification.

[4] Satellite observations are often the only available means for estimating TC intensity. Unlike infrared sensors, passive microwave channels allow penetration into precipitating clouds, therefore providing information about precipitation and ice particles instead of just the cloud tops. This study uses the 37 GHz frequency measurements, which detect both emission from liquid hydrometeors and scattering of upwelling radiation by cloud ice [*Weng and Grody*, 1994]. The findings documented here represent the first time that the 37 GHz ring pattern in the inner core is identified as a specific and unique feature that is associated with TC RI, and in such cases immediately precedes eyewall development.

2. Data and Methods

[5] To examine TC precipitation morphology during periods of RI, a set of images is collected of all TC satellite overpasses during 2003–2007 in the North Atlantic basin from the 37 GHz color composite product provided by the Navy Research Laboratory (NRL) TC satellite web page (http://www.nrlmry.navy.mil/TC.html) [*Hawkins et al.*, 2001; *Hawkins and Velden*, 2011]. The 37 GHz is used here for its capacity of detecting low-level circulation centers, which are sometime unseen at 85 GHz [*Lee et al.*, 2002; *Turk et al.*, 2006]. In order to better display the 37 GHz observations including its sensitivity for both low-level clouds and deep convection, the 37 GHz color composite (hereafter 37color) product was developed at NRL for real-time TC image

[1]Department of Earth and Environment, Florida International University, Miami, Florida, USA.

Corresponding author: H. Jiang, Department of Earth and Environment, Florida International University, 11200 SW 8th St., PC-342B, Miami, FL 33199, USA. (haiyan.jiang@fiu.edu)

Table 1. List of Three RI Events of Hurricane Emily (2005)

	Time (mmddhh)	Initial Intensity (kt)	Intensity Increase During the Next 24-h
Event #1	071306	45	30
	071312	50	35
	071318	55	45
	071400	70	40
	071406	75	40
	071412	85	30
Event #2	071518	95	40
	071600	110	30
Event #2	071900	75	35
	071906	80	30

distribution [*Lee et al.*, 2002]. It is constructed by using 37 GHz vertically polarized (V37) and horizontally polarized (H37) brightness temperatures, and polarization correction temperature (PCT37 [*Cecil et al.*, 2002]). The ocean surface appears cold in V37 and H37, similar to ice-scattering in deep convection which also appears cold in both V37 and H37. To correct this ambiguity, the PCT37 is defined by PCT37 = $2.18 \times 37V - 1.18 \times H37$. The resulting PCT37 is cold for ice-scattering and warm for the ocean surface. The 37color product implements a red/green/blue color composite from PCT37, H37 and V37 so that qualitatively the ocean surface in the color product appears dark green, deep convection appears pink, and low-level water clouds and warm rain appear cyan. The quantitative information is sacrificed. The 37color product is generated for all TC overpasses from the Tropical Rainfall Measuring Mission (TRMM) Microwave Imager (TMI), Advanced Microwave Scanning Radiometer for EOS (AMSR-E), WindSat, Special Sensor Microwave Imager (SSM/I), and Special Sensor Microwave Imager/Sounder (SSMIS) when these data are available.

[6] After examining many 37color images of the entire life cycle of TCs, we hypothesize that the first appearance of a well-defined cyan color ring pattern in the inner core immediately surrounding the warm center is associated with RI. The purpose of this study is to test this hypothesis. Using the 37color images collected for 84 named TCs during 2003–2007 hurricane seasons in the North Atlantic basin, the ring pattern is searched for within each satellite overpass that captures the TC inner core. The following criteria are used to define a ring pattern: 1) It immediately surrounds the warm center of the developing TC; 2) It is symmetric (round) and should be at least 90% closed (not a partial ring); 3) The minimum thickness between the inner and outer edges of the ring should be at least one-fourth of the diameter of the outer edges; 4) The ring should consist of mostly solid bright cyan and not a faded cyan; 5) Part of the ring could be pink (intense convection overlaying cyan ring).

[7] The best track data from the National Hurricane Center (NHC) are used to determine RI cases from the 84 TCs. *RI cases* are defined as those cases with 24-hour maximum wind speed intensity increase equal to or greater than 30 kt [*Kaplan and DeMaria*, 2003]. From the best track data, a 24-hour period beginning at each synoptic time (i.e., 0000, 0600, 1200 and 1800 UTC) is considered the starting point of one potential RI case. Therefore consecutive RI cases each overlap by 18 hours. To be included in the study, the inner core of the TC must be over water for the period of RI. The initial intensity must be less than or equal to 100 kt. The 84 TCs contributed a total of 1735 cases (i.e., 24-h periods with initial time at the 6 hourly synoptic times). When environmental conditions are favorable for RI, in many instances the favorable environment exists for a day or so, so that when a TC starts to rapidly intensify, the intensification continues for at least 24 hours and can last as long as 48–60 hours. Here we define this period of RI as one *RI event*. Using the definition of RI as an increase of 30 kt or higher in 24 hours, with best track data for every 6-hour synoptic time, each RI event can be defined as a cluster of *continuous and overlapping* 24-hr *RI cases*. RI events in the study contained up to 6 overlapping RI cases, and each TC could have more than one RI event. For example, as shown in Table 1, Hurricane Emily (2005) experienced three RI events. The first RI event has 6 overlapping RI cases. The second and third events, both of which consist of two overlapping RI cases, began after the storm subsequently weakened. In this study, a ring pattern is searched from all the available 37color images with observation times within $t - 5$ h and $t + 1$ h (t is the initial time of each 6-h case). According to discussions with NHC forecasters, up to one hour delay of the microwave data is acceptable to be used in their forecasts. Since our hypothesis is that only the first ring occurrence during each RI event can be use as a predictor, here only the first ring during each TC intensifying period is counted and recorded. The Statistical Hurricane Intensity Prediction Scheme (SHIPS) RI index (RII) [*Kaplan et al.*, 2010] is used to evaluate the environmental factors for each best track case. The SHIPS RII probability values for a 30 kt intensity increase during 24 h (hereafter RII_30 kt) are obtained from the post-time dependent run of the most recent version of SHIPS RII algorithm for 1995–2010 storms. These values are matched with the 6-hourly best track data. One caveat is that there are 762 out of 1735 total cases with no SHIPS RII available due to either extra-tropical condition or low initial storm intensity. In the remaining 973 cases, there are 195 cases with no 37 GHz satellite data available. Therefore, the final total number of qualified cases used in this study is 778. There are 71 actual RI cases out of these 778 cases and these 71 RI cases are from 28 RI events. The total number of RI cases during 2003–2007 Atlantic hurricane seasons is 104 (including 7 overland RI cases) from 31 RI events.

3. Results and Discussion

[8] Identifying ring patterns in the 37color images mainly relies on higher resolution sensors including TMI, AMSR-E, and WindSat, although lower resolution sensors including SSM/I and SSMIS can be used for storms with very large eyes. Figure 1 shows an example of the ring feature, an NRL 37color image from a WindSat overpass at 11:05 UTC October 18, 2005 associated with a record-setting RI event for Hurricane Wilma (2005). The first ring pattern during each TC intensifying period occurred in 45 out of the 778 cases (Table 2). In the 45 possible RI cases with a ring, there are 23 cases that actually went through RI. There are 19 out of these 23 cases in which a ring pattern appeared during $t - 5$ h and $t + 1$ h period, but four other cases had a ring pattern more than one hour after the starting time of the 24-h RI period. In real-time NHC forecasts, these 4 RI cases will be missed if using the ring pattern as a predictor.

[9] The ring pattern also appeared at the beginning of 22 intensifying cases that did not go through RI (Table 2). There were no differences in the appearance of the ring

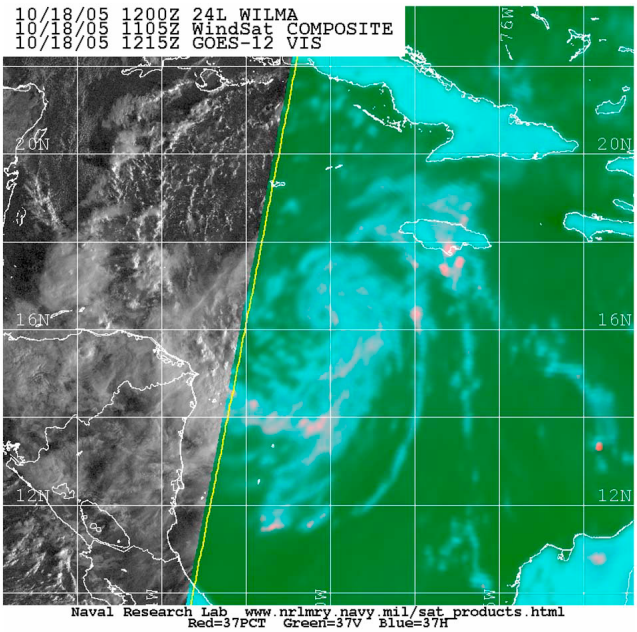

Figure 1. An example of a precipitative ring in Hurricane Wilma (2005)'s NRL 37color image from a WindSat overpass at 11:05 UTC October 18, 2005. The ring pattern occurred about one hour before an RI case with a 24-h intensity increase of 95 kts. Courtesy of the Naval Research Laboratory (NRL) TC satellite web page (http://www.nrlmry.navy.mil/TC.html). (Note that if you are reading a printed copy of the figure, the cyan color might not be as clear as in the electronic copy viewed from a computer screen).

pattern between cases that went through RI and those that did not. It is likely that all TCs at this point had reached a similar stage in their core development, but the environmental factors are different for these RI and non-RI cases. The SHIPS RII probability for a 30 kt increase in 24-h (RII_30 kt [*Kaplan et al.*, 2010]) is examined. The RII-30 kt values are probabilities scaled from 0 to 100%, with the higher values indicating higher probabilities of RI due to favorable environmental conditions. It is found that the average SHIPS RII-30 kt is much higher for RI cases (27.5%) than non-RI cases (4.5%). If an arbitrary threshold of RII-30 kt is selected to be ≥5% for a favorable environment, 21 out of 23 RI cases satisfies this threshold and all but 2 non-RI cases do not meet this threshold. The 20 non-RI cases with a ring and SHIPS RII-30 kt < 5% are correct rejections, but the 2 non-RI cases with a ring and SHIPS RII-30 kt ≥ 5% are false alarms. In the 23 RI cases, there are 17 correct forecast (hit) cases (with ring during t − 5 h and t + 1 h and SHIPS_RII ≥ 5%), 4 microwave late cases (with ring during t + 1 h and t + 7 h and SHIPS_RII ≥ 5%), and 2 misses (with ring during t − 5 h and t + 1 h and SHIPS RII < 5%, see Table 2). Therefore the SHIPS RII can be used as a discriminator for RI and non RI cases, even though both cases have a ring feature.

[10] Based on the result shown in Table 2, the probability of RI if using the 37 GHz ring as the sole criterion (the ring RI index) is 38% (17/45, Table 3). This represents a factor of 5.4 increases from the climatological mean during the same 5-yr period. *Jiang* [2012] indicated that the probability of RI for TCs with hot towers in the inner-core is 9.6%, which is only about a factor of 1.5 increases from the climatological mean (6.3%) using TRMM precipitation radar observed TCs during 1998–2008. Although *Jiang*'s [2012] results are for global TCs, the substantial difference with this study demonstrates that the ring pattern might be a better inner-core process related indicator for the RI prediction.

[11] The SHIPS RII probability threshold used to forecast RI is about 20% for the Atlantic basin [*Kaplan et al.*, 2010]. Here we use this threshold to evaluate the probability of RI for the SHIPS RII. There are 163 cases with RII_30 kt ≥ 20%, in which there are 55 actual RI cases. Therefore, the probability of RI is 34% (55/163, Table 3), which is slightly lower than the probability of RI for the ring RI index (38%). This indicates that environmental conditions and inner-core properties might weight almost equally in terms of determining RI, although other inner-core processes need to be taken into account as well besides the ring pattern.

[12] Since a favorable environment condition is necessary for RI, it is optimal to add the SHIPS RII criterion to the ring RI index (RII). Here it is decided to use RII_30 kt ≥ 5% as the additional criterion besides the ring. We call this combined RI index Ring+SHIPS RII. As shown in Table 3, there are 23 (out of 778) cases that satisfy the ring and RII_30 kt ≥ 5% criteria, in which there are 17 actual RI cases. This produces a probability of RI of 74% (17/23), which is about a factor 2 higher than the probability of either the ring or SHIPS RII alone. This indicates that the 37 GHz ring RII and SHIPS RII are independent predictors. This indicates that RI is dependent on favorable conditions and a certain level of internal core structure to a similar extent, and that symmetric warm rain (indicated by the cyan color ring on the 37 GHz product) is an important element in this core structure.

[13] The probability of detection (POD) and false alarm ratio (FAR) for 2003–2007 storms are also shown in Table 3. The POD is the percentage of RI cases that are correctly identified. The FAR is the number of times that RI is forecasted but does not occur divided by the total number of times RI is forecast. The FAR is equal to one minus the probability of RI. The PODs for the ring only, SHIPS RII only, and ring+SHIPS RII are 24% (17/71), 77% (55/71), and 24% (17/71), respectively. The POD for the combined RII is a factor of 3 lower than that for the SHIPS RII. The FARs for the ring only, SHIPS RII only, and ring+SHIPS RII are 62%, 66%, and 26%. The FAR for the combined RII is a factor of 2.5 lower than that for the SHIPS RI. This shows that the ring+SHIPS RII has a great potential to reduce the false alarm rate, but the detection rate is somewhat sacrificed when treating every 6-h synoptic time as one case.

[14] As mentioned above, RI usually happens as an event, noted in the best track data as a cluster of continuous and overlapping 24-h RI cases. Hurricane forecasters often prefer to characterize RI as an event. The ring+SHIPS RI forecast scheme was initially designed as an event-based forecast method. From this point of view, a separate statistic is done to evaluate the method based on RI events using the 2003–2007 Atlantic hurricane seasons. As listed in Table 4, there are a total of 28 RI events associated with 24 TCs: 21 hits and 7 misses. The ring+SHIPS RII forecast method captures 21 out of these 28 events, producing a POD of 75% (21/28). Two events are missed due to a low SHIPS RII value, and five events are missed due to a lack of a ring feature. After taking the two false alarm cases in Table 2 into account, the FAR is 9% (2/23), which corresponds to a 91% probability of RI. This extremely high performance comes with three

Table 2. List of RI (23) and Non-RI (22) Cases Having the First 37 GHz Ring Pattern Occurring During the Intensification Stages of TCs in the 2003–2007 Atlantic Hurricane Seasons[a]

Number	Storm	Best Track Starting Time and Intensity (kt)	Best Track Ending Time	Time of Microwave Overpass With Ring Pattern	Intensity Change in 24 h (kt)	RII_30 kt (%)
	RI Cases With a Ring Between t − 5 h and t + 1 h (t is the RI Initial Time) and SHIPS_RII_30 kt ≥ 5% (17 Hits)					
1	2003 Fabian	08/30 06Z, 70 kt	08/31 06Z	08/30 0217Z TRMM	40	22
2	2003 Isabel	09/07 12Z, 65 kt	09/08 12Z	09/07 0906Z SSM/I	45	39
3	2004 Alex	08/02 18Z, 50 kt	08/03 18Z	08/02 1312Z SSMI	35	20
4	2004 Danielle	08/14 18Z, 55 kt	08/15 18Z	08/14 1527Z TRMM	30	33
5	2004 Frances	08/26 12Z, 55 kt	08/27 12Z	08/26 1049Z TRMM	35	47
6	2004 Ivan	09/05 00Z, 60 kt	09/06 00Z	09/04 2043Z WindSat	55	23
7	2004 Jeanne (2)	09/19 18Z, 45 kt	09/20 18Z	09/19 1824Z AMSR-E	30	16
8	2005 Dennis (1)	07/07 12Z, 90 kt	07/08 12Z	07/07 0542Z TRMM	40	32
9	2005 Emily (1)	07/14 12Z, 85 kt	07/15 12Z	07/14 1037Z WindSat	30	30
10	2005 Emily (3)	07/19 00Z, 75 kt	07/20 00Z	07/18 2359Z WindSat	35	22
11	2005 Katrina	08/27 06Z, 95 kt	08/28 06Z	08/27 1942Z AMSR-E	50	23
12	2005 Rita	09/20 18Z, 85 kt	09/21 18Z	09/20 1500Z TRMM	60	31
13	2005 Wilma	10/18 06Z, 60 kt	10/19 06Z	10/18 1105Z WindSat	85	50
14	2006 Helene	09/17 00Z, 70 kt	09/18 00Z	09/16 2026Z WindSat	30	23
15	2007 Dean (1)	08/15 12Z, 50 kt	08/16 12Z	08/15 1105Z SSM/I	30	16
16	2007 Dean (2)	08/17 12Z, 90 kt	08/18 12Z	08/17 1220Z SSMIS	55	46
17	2007 Felix	09/02 00Z, 65 kt	09/03 00Z	09/01 2148Z WindSat	85	36
	RI Cases With a Ring After t + 1 h (t is the RI Initial Time) and SHIPS_RII_30 kt ≥ 5% (4 Late Cases)					
1	2004 Karl	09/17 18Z, 55 kt	09/18 18Z	09/17 2317Z TRMM	40	43
2	2004 Lisa	09/20 06Z, 30 kt	09/21 06Z	09/20 0818Z WindSat	30	16
3	2006 Florence	09/09 18Z, 50 kt	09/10 18Z	09/09 2001Z TRMM	30	31
4	2006 Gordon	09/13 06Z, 70 kt	09/14 06Z	09/13 1005Z WindSat,	35	21
	RI Cases With a Ring Between t − 5 h and t + 1 h (t is the RI Initial Time) and SHIPS_RII_30 kt < 5% (2 Misses)					
1	2005 Dennis (2)	07/09 12Z, 80 kt	07/10 12Z	07/09 1202Z WindSat	40	3
2	2005 Emily (2)	07/15 18Z, 95 kt	07/16 18Z	07/15 1801Z AMSR-E	40	3
	Non-RI Cases With a Ring and SHIPS_RII_30 kt < 5% (20 Correct Rejections)					
1	2003 Ana	04/22 00Z, 50 kt	04/23 00Z	04/21 2338Z TMI	−10	3
2	2003 Danny	07/18 06Z, 55 kt	07/19 06Z	07/18 0558Z TRMM	10	3
3	2003 Juan	09/26 18Z, 70 kt	09/27 18Z	09/26 1639Z TRMM	20	3
4	2003 Kate	10/01 18Z, 65 kt	10/02 18Z	10/01 1659Z TRMM	15	3
5	2004 Alex (2)	08/04 06Z, 80 kt	08/05 06Z	08/04 0316Z TRMM	25	3
6	2004 Lisa (1)	09/21 06Z, 60 kt	09/22 06Z	09/21 0401Z AMSR-E	−10	3
7	2004 Lisa (2)	10/02 00Z, 60 kt	10/03 00Z	10/01 2008Z TRMM	−10	3
8	2005 Irene (1)	08/12 00Z, 45 kt	08/13 00Z	08/11 2201Z WindSat	15	3
9	2005 Irene (2)	08/15 12Z, 75 kt	08/16 12Z	08/15 0720Z TRMM	10	3
10	2005 Nate	09/07 18Z, 70 kt	09/08 18Z	09/07 1540Z TRMM	5	3
11	2005 Ophelia(1)	09/10 18Z, 70 kt	09/11 18Z	09/10 1428Z TRMM	−5	3
12	2005 Ophelia(2)	09/12 18Z, 60 kt	09/13 18Z	09/12 1730Z TRMM	0	3
13	2005 Vince	10/09 00Z, 45 kt	10/10 00Z	10/08 2133Z TRMM	15	3
14	2005 Epsilon(1)	12/03 00Z, 65 kt	12/04 00Z	12/02 1942Z TRMM	0	3
15	2005 Epsilon(2)	12/04 00Z, 65 kt	12/05 00Z	12/03 1847Z TRMM	5	3
16	2005 Delta	11/24 00Z, 55 kt	11/24 00Z	11/23 2131Z TRMM	5	3
17	2005 Zeta	12/30 12Z, 45 kt	12/31 12Z	12/30 0807Z WindSat	5	3
18	2006 Debby	08/23 06Z, 40 kt	08/24 06Z	08/23 0125Z TRMM	5	3
19	2006 Gordon(2)	09/17 18Z, 70 kt	09/18 18Z	09/17 1736Z TRMM	15	3
20	2006 Isaac	09/28 12Z, 40 kt	09/29 12Z	09/28 1040Z TRMM	5	3
	Non-RI Cases With a Ring and SHIPS_RII_30 kt ≥ 5% (2 False Alarms)					
1	2004 Ivan (2)	09/07 06Z, 95 kt	09/08 06Z	09/07 0528Z AMSR-E	25	16
2	2005 Maria	09/05 00Z, 75 kt	09/06 00Z	09/04 2007Z TRMM	25	23

Table 3. Probability of RI for 2003–2007 Atlantic TCs Using the Ring, SHIPS RII, and Ring+SHIPS RII Criteria for the 30-kt RI Threshold

	Climatological Mean	Ring	SHIPS RII ≥ 20%	Ring+SHIPS RII ≥ 5%
# of total forecasts	778	45	163	23
# of correct forecasted cases	71	17	55	17
Probability of RI	9%	38%	34%	74%
POD	100%	24%	77%	24%
FAR (=1 − Probability of RI)	91%	62%	66%	26%

Table 4. List of All Best Track RI Events (28) During 2003–2007 Hurricane Seasons in the Atlantic Basin[a]

Number	Storm	Best Track RI Starting Time and Intensity (kt)	Total RI Event Duration (h)	Number of RI Cases in the RI Event	Hours From the RI Starting Time to Ring Time (h)	Hours From Ring Time to the RI Ending Time (h)	Total Intensity Increase During the RI Event	24-h Intensity Increase Associated With the Ring (kts)	Highest 24-h Intensity Increase During the RI Event (kts)
21 RI Events With Ring and SHIPS_RII_30 kt > 5% (RI Was Indicated and RI Occurred)									
1	2003 Fabian	08/29 12Z, 50	42	4	14.5	27.5	60	40	45
2	2003 Isabel	09/07 06Z, 60	42	4	3	39	55	45	45
3	2004 Alex	08/02 06Z, 40	36	3	7	29	45	35	35
4	2004 Danielle	08/14 00Z, 35	42	4	15.5	26.5	50	30	35
5	2004 Frances	08/25 18Z, 35	54	6	17	37	65	35	35
6	2004 Ivan	09/05 00Z, 60	42	4	9	31	60	55	55
7	2004 Jeanne	09/19 18Z, 45	24	1	0.5	23.5	30	30	30
8	*2004 Karl*	*09/17 00Z, 40*	*42*	*4*	*23.5*	*18.5*	*55*	*40*	*40*
9	*2004 Lisa*	*09/20 06Z, 30*	*24*	*1*	*2.5*	*21.5*	*30*	*30*	*30*
10	2005 Dennis (1)	07/06 06Z, 50	54	6	23.5	30.5	75	30	50
11	2005 Emily (1)	07/13 06Z, 45	54	6	28.5	25.5	70	30	45
12	2005 Emily (3)	07/19 00Z, 75	30	2	0	30	35	35	35
13	2005 Katrina	08/27 06Z, 95	42	4	13.5	28.5	55	40	50
14	2005 Rita	09/20 00Z, 60	54	6	15	34	95	60	60
15	2005 Wilma	10/17 18Z, 45	48	5	17	30	105	95	95
16	*2006 Florence*	*09/09 18Z, 50*	*24*	*1*	*2*	*22*	*30*	*30*	*30*
17	*2006 Gordon*	*09/12 12Z, 50*	*42*	*4*	*22*	*20*	*55*	*35*	*35*
18	2006 Helene	09/17 00Z, 70	30	2	−3.5	26.5	35	30	30
19	2007 Dean (1)	08/15 12Z, 50	24	1	−3	21	30	30	30
20	2007 Dean (2)	08/16 18Z, 80	42	4	18.5	23.5	65	55	65
21	2007 Felix	08/31 18Z, 30	60	7	22	38	105	85	85
2 RI Events With Ring and SHIPS_RII_30 kt < 5% (RI Not Indicated by Low SHIPS RII, but RI Occurred)									
22	*2005 Dennis (2)*	*07/09 06Z, 75*	*30*	*2*	*6*	*24*	*55*	*40*	*50*
23	*2005 Emily (2)*	*07/15 18Z, 95*	*30*	*2*	*0*	*30*	*45*	*40*	*40*
	Mean		***40***	***3.6***	***11***	***29***	***53***	***42***	***46***
5 RI Events Without Ring (RI Not Indicated by Lack of Ring Feature, but RI Occurred)									
24	2005 Cindy	07/04 18Z, 30	30	2	N/A	N/A	35	N/A	35
25	2005 Stan	10/03 06Z, 35	24	1	N/A	N/A	30	N/A	30
26	2005 Beta	10/29 06Z, 70	30	2	N/A	N/A	40	N/A	30
27	2007 Karen	09/25 12Z, 35	30	2	N/A	N/A	30	N/A	30
28	2007 Lorenzo	09/26 12Z, 30	30	2	N/A	N/A	40	N/A	40

[a]The best track RI starting time and intensity, total RI event duration, hours from the RI starting time to the RI ring time, hours from the ring time to the RI ending time, total intensity increase during the RI event, 24-h intensity increase associated with the ring, and the highest 24-h intensity increase during the RI event are indicated.

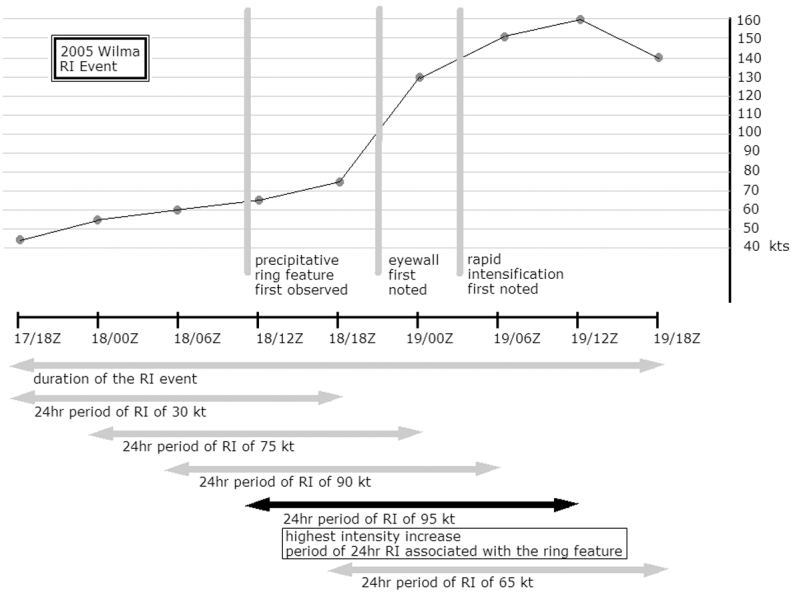

Figure 2. Time series of the 6 hourly best track maximum wind speed (in kts) of Hurricane Wilma (2005) during its 48-h RI event between 18Z October 17 and 18Z October 19. The times of the first ring feature seen in the 37color product, eyewall first noted by NHC in the advisory package, and RI first noted by NHC in the advisory package are indicated as vertical lines. Five overlapping 24-h periods of RI are indicated as arrows at the bottom of the figure. The ring was observed over 24 hours prior to the observation that the hurricane was going through an RI event.

compromises. First, the method usually does not detect the onset of the RI event, instead identifying one 24-hour period in the middle of the RI event. As seen in the fourth column of Table 4 (hours from the RI starting time to ring time), only 3 of the 21 captured RI events show that the ring appeared on or before the RI starting time. On average, the total RI event duration is 40 hours for the 23 RI events with rings. The ring appears 11 hours after the onset of RI on average. Second, due to microwave latency, lack of timely microwave passes over the center of the TC, lack of a higher-resolution pass over a TC with a small center, or a delayed onset of the ring feature associated with a moderately sheared environment, there are some late cases in which the period from the ring time to the RI ending time is less than 24 hours. There are 8 out of the 23 ring cases with hours from the ring time to the RI ending time less than 24 hours. Third, the method forecasts once for each RI event. As seen in the third column of Table 4, the number of overlapping RI cases (note that each case is one 24-h period of RI starting at 6 hourly synoptic times) in each RI event is usually greater than one. On average, the number is 3.6. Therefore, the method will miss about 72% of RI cases if evaluating it based on RI cases instead of RI events. This is reflected in the POD of 24% in Table 3 based on RI cases.

[15] Advantages that makes a strong argument for using the ring+SHIPS RII forecast method can be seen in Figure 2, which shows an example of Hurricane Wilma (2005)'s RI event between 18Z October 17 and 18Z October 19. The 48-h RI event contains five overlapping 24-h RI cases. The SHIPS RII_30 kt gives greater than 20% values for all these five cases, so it would technically forecast five hits for this one 48-hour RI event. The ring+SHIPS RII forecasts once at 12Z October 18 based on the ring pattern seen by a WindSat overpass at 11:05 UTC October 18 (Figure 1), Therefore, the ring+SHIPS RII misses 4 out of 5 RI cases. However, it catches the RI case with highest intensity increase (24 hour intensity increase of 95 kt) of the five overlapping RI cases. The ring feature occurs prior to significant intensity increases, when there is also no indication from the conventional satellite imagery that Wilma is about to begin a period of RI, during what appears to be a period of gradual intensification. The first ring occurs prior to eyewall development and well in advance of the first mention of a period of RI in the NHC forecast discussions. It is the only early clue to the period of RI that is about to begin, and the transition from a Category 1 hurricane to a Category 5 hurricane in the subsequent 24 hours. The ability of the ring feature to precisely pinpoint large intensity increases should prove advantageous for improving intensity forecast performance.

[16] Statistics on these intensity increases for the RI events of 2003–2007 are presented in the last three columns of Table 4. The average total intensity increase during the 23 RI events with ring features is 53 kt, and the ring+SHIPS RII captures 43 kt of that on average, which is 79% of the total intensity increase for the RI event. The average highest 24-h intensity increase is 46 kt, which is only 3 kt higher than that captured by the method. By comparing the 7th and 8th columns of Table 4, we can see that the 37 GHz ring is associated with the highest 24-h intensity increase for 16 out 23 RI events with rings. For the remaining 7 RI events, timing or lack of good microwave passes over the center might be a factor for the miss.

4. Conclusions

[17] Using the NRL 37color product during 2003–2007 for 84 TCs in the Atlantic basin, it is found that the first appearance of a cyan color ring around the storm center is associated with the subsequent storm rapid intensification

when environmental conditions are favorable for development. A simple subjective technique for predicting RI in the next 24 hours is proposed using both the 37 GHz ring pattern and the SHIPS RII for TCs with intensity ≤100 kt that are currently over water and are anticipated to remain over water for the next 24 hours. For the 84 TCs used in this study, this ring+SHIPS RI forecast method produces a probability of RI of 74%, which is about a factor of two higher than that for either of the ring or SHIPS RII. This indicates that the 37 GHz ring RII and SHIPS RII are independent predictors. Both the POD and FAR for the combined ring+SHIPS RII are lower than those for SHIPS RII alone (POD, 24% versus 77%, and FAR, 26% versus 66%) when treating every 6-hr synoptic time as a separate case.

[18] Because the method was initially developed for RI event-based forecasts, a verification based on 2003–2007 Atlantic RI events is performed. The method captures 21 out of these 28 events, producing a POD of 75% and a FAR of only 9%. This extremely high performance comes with three compromises: 1) the method usually does not detect the onset of the RI event, instead identifying one 24-hour period in the middle of the RI event; 2) due to microwave latency, lack of timely microwave passes over the center of the TC, lack of a higher-resolution pass over a TC with a small center, or a delayed onset of the ring feature associated with a moderately sheared environment, there are some late cases in which the period from the ring time to the RI ending time is less than 24 hours; 3) the method forecasts once for each RI event, which means that typically half to three quarters of overlapping 24-h RI cases will be missed if evaluating RI based on 24-hour RI cases instead of RI events. Major advantages of using the 37 GHz ring pattern to forecast an RI event are: 1) NHC forecasters usually couch rapid intensification in terms of an RI event in the forecast discussion of the advisory package, even though quantitative intensity increases are forecast; 2) the ring precedes observations that an RI event is in progress by at least 24 hours, well before any significant intensity increases, and before the TC appears to be intensifying on conventional Infrared satellite imagery; 3) this forecast method is often found to be associated with the highest intensity increase of the overlapping RI cases associated with the RI event; 4) the ring feature is often a hallmark of intensification to major hurricane; and 5) the ability of the forecast method to pinpoint large intensity increases should benefit the performance of intensity forecasting, which has consistently lagged behind track forecast performance improvements. Future study will focus on automating the ring identifying procedure in order to transfer the forecast method from subjective to objective. Study is also underway to analyze what is in the cyan ring using the three-dimensional observations of the TRMM Precipitation Radar.

[19] **Acknowledgments.** The authors acknowledge the Naval Research Laboratory's (NRL) Marine Meteorology Division for maintaining the NRL TC satellite webpage. Huge thanks go to John Kaplan for providing SHIPS RII data. Thanks to Jack Beven, John Knaff, James Franklin, Frank Marks, John Molinari, Mike Montgomery, Ed Zipser, Dave Roberts, Eric Blake and Todd Kimberlain for suggestions, comments, support, and encouragement for this work. The authors also would like to give acknowledgments to John Kaplan and another anonymous reviewer, whose comments helped improve the manuscript substantially. Support for this study is provided by the NOAA Joint Hurricane Testbed (JHT) grant (NA11OAR4310193) and NASA Hurricane Science Research Program (HSRP) grant (NNX10AG34G). The first author received support from the Florida International University Presidential Fellowship, and the second author received support from NASA New Investigator Program (NIP) award (NNX10AG55G).

[20] The Editor thanks the two anonymous reviewers for assisting in the evaluation of this paper.

References

Braun, S. A., M. T. Montgomery, and Z. Pu (2006), High-resolution simulation of Hurricane Bonnie (1998). Part I: The organization of eyewall vertical motion, *J. Atmos. Sci.*, *63*, 19–42, doi:10.1175/JAS3598.1.

Cecil, D., E. J. Zipser, and S. W. Nesbitt (2002), Reflectivity, ice scattering, and lightning characteristics of hurricane eyewalls and rainbands. Part I: Quantitative description, *Mon. Weather Rev.*, *130*, 769–784, doi:10.1175/1520-0493(2002)130<0769:RISALC>2.0.CO;2.

Hawkins, J. D., and C. Velden (2011), Supporting meteorological field experiment missions and post-mission analysis with satellite digital data and products, *Bull. Am. Meteorol. Soc.*, *92*, 1009–1022, doi:10.1175/2011BAMS3138.1.

Hawkins, J. D., T. F. Lee, F. J. Turk, C. Sampson, J. Kent, and K. Richardson (2001), Real-time Internet distribution of satellite products for tropical cyclone reconnaissance, *Bull. Am. Meteorol. Soc.*, *82*, 567–578, doi:10.1175/1520-0477(2001)082<0567:RIDOSP>2.3.CO;2.

Hendricks, E. A., M. S. Peng, B. Fu, and T. Li (2010), Quantifying environmental control on tropical cyclone intensity change, *Mon. Weather Rev.*, *138*, 3243–3271, doi:10.1175/2010MWR3185.1.

Jiang, H. (2012), The relationship between tropical cyclone rapid intensification and the strength of its convective precipitation features, *Mon. Weather Rev.*, *140*, 1164–1176, doi:10.1175/MWR-D-11-00134.1.

Kaplan, J., and M. DeMaria (2003), Large-scale characteristics of rapidly intensifying tropical cyclones in the North Atlantic basin, *Weather Forecast.*, *18*, 1093–1108, doi:10.1175/1520-0434(2003)018<1093:LCORIT>2.0.CO;2.

Kaplan, J., M. DeMaria, and J. A. Knaff (2010), A revised tropical cyclone rapid intensification index for the Atlantic and eastern North Pacific basins, *Weather Forecast.*, *25*, 220–241, doi:10.1175/2009WAF2222280.1.

Lee, T. F., F. J. Turk, J. Hawkins, and K. Richardson (2002), Interpretation of TRMM TMI images of tropical cyclones, *Earth Interact.*, *6*, 1–17, doi:10.1175/1087-3562(2002)006<0001:IOTTIO>2.0.CO;2.

Malkus, J. S., C. Ronne, and M. Chaffee (1961), Cloud patterns in Hurricane Daisy, 1958, *Tellus, Ser. A*, *13*, 8–30, doi:10.1111/j.2153-3490.1961.tb00062.x.

Merrill, R. T. (1988), Environmental influences on hurricane intensification, *J. Atmos. Sci.*, *45*, 1678–1687, doi:10.1175/1520-0469(1988)045<1678:EIOHI>2.0.CO;2.

Molinari, J., and D. Vollaro (2010), Rapid intensification of a sheared tropical storm, *Mon. Weather Rev.*, *138*, 3869–3885, doi:10.1175/2010MWR3378.1.

Montgomery, M. T., M. E. Nicholls, T. A. Cram, and A. B. Saunders (2006), A vortical hot tower route to tropical cyclogenesis, *J. Atmos. Sci.*, *63*, 355–386, doi:10.1175/JAS3604.1.

Nguyen, C. M., M. J. Reeder, N. E. Davidson, R. K. Smith, and M. T. Montgomery (2011), Inner-core vacillation cycles during the intensification of Hurricane Katrina, *Q. J. R. Meteorol. Soc.*, *137*, 829–844, doi:10.1002/qj.823.

Nolan, D. S., and L. D. Grasso (2003), Nonhydrostatic, three-dimensional perturbations to balanced, hurricane-like vorticies. Part II: Symmetric response and nonlinear simulations, *J. Atmos. Sci.*, *60*, 2717–2745, doi:10.1175/1520-0469(2003)060<2717:NTPTBH>2.0.CO;2.

Rappaport, E. N., et al. (2009), Advances and challenges at the National Hurricane Center, *Weather Forecast.*, *24*, 395–419, doi:10.1175/2008WAF2222128.1.

Shapiro, L. J., and H. E. Willoughby (1982), The response of balanced hurricanes to local sources of heat and momentum, *J. Atmos. Sci.*, *39*, 378–394, doi:10.1175/1520-0469(1982)039<0378:TROBHT>2.0.CO;2.

Simpson, J., J. B. Halverson, B. S. Ferrier, W. A. Peterson, R. H. Simpson, R. Blakeslee, and S. L. Durden (1998), On the role of "hot towers" in tropical cyclone formation, *Meteorol. Atmos. Phys.*, *67*, 15–35, doi:10.1007/BF01277500.

Turk, F. J., S. DiMichele, and J. D. Hawkins (2006), Observations of tropical cyclone structure from WindSat, *IEEE Trans. Geosci. Remote Sens.*, *44*(3), 645–655, doi:10.1109/TGRS.2006.869926.

Weng, F., and N. C. Grody (1994), Retrieval of cloud liquid water using the special sensor microwave imager (SSM/I), *J. Geophys. Res.*, *99*(D12), 25,535–25,551.

Willoughby, H. E. (1990), Temporal changes of the primary circulation in tropical cyclones, *J. Atmos. Sci.*, *47*, 242–264, doi:10.1175/1520-0469(1990)047<0242:TCOTPC>2.0.CO;2.

Willoughby, H. E., J. A. Clos, and M. B. Shoreibah (1982), Concentric eyewalls, secondary wind maxima, and the development of the hurricane vortex, *J. Atmos. Sci.*, *39*, 395–411, doi:10.1175/1520-0469(1982)039<0395:CEWSWM>2.0.CO;2.